COMPARATIVE KINETIC ANALYSIS OF VIRE2 INTRACELLULAR TRAFFICKING

YU TAIAN

NATIONAL UNIVERSITY OF SINGAPORE

2015

COMPARATIVE KINETIC ANALYSIS OF VIRE2 INTRACELLULAR TRAFFICKING

YU TAIAN
(B. ENG. (HONS.), CAU)

A THESIS SUBMITTED

FOR THE DEGREE OF MASTER OF SCIENCE
DEPARTMENT OF CHEMISTRY
NATIONAL UNIVERSITY OF SINGAPORE

2015

DECLARATION

I hereby declare that this thesis is my original work and it has been written by me in its entirety. Under the supervision of A/P Pan Shen Quan, (in the laboratory S1A #06-20), Department of Biological Sciences, National University of Singapore, between 3 Aug 2014 and 3 Aug 2015.

I have duly acknowledged all the sources of information which have been used in the thesis.

This thesis has also not been submitted for any degree in any university previously.

Yu Taian		
Name	Signature	Date

ACKNOWLEDGEMENTS

First of all, I would like to express my deepest gratitude and appreciation to my supervisor, Associated Professor Pan Shen Quan for his close supervision throughout the entire project. From the planning to the execution of my project, a lot of effort was taken to ensure that I would be exposed to different techniques and fields of the lab. I am blessed to be part of Prof Pan's team where my learning was always the main priority.

My sincere appreciation goes to Dr. Yang Qinghua who patiently guided me in my experiments and thesis writing. I would like to thank him for the effort and time he has taken to introduce me to the field of biological science. His teachings go beyond that of experimental techniques and scientific papers. From him, I have also learned the right attitude and thinking that a scientist should have while doing research.

I would also wish to thank the other members of the lab, Haitao, Peng Ling, Zijie, Xiaoyang and Sangram for their help and advice. Also, a big thank you to all the staff of Department of Biological Sciences for all the assistance they provided.

Lastly, I would like to extend my heartfelt gratitude to my family and friends for their unwavering support and concern throughout my study period in Singapore.

TABLE OF CONTENTS

SUMMARY

Previous studies in this lab revealed that the trafficking of bacterium-originated VirE2 is driven by an actomyosin motility system in the tobacco leaf epidermal cells. This trafficking manner closely resembles some of plant organelles. Although the mechanisms of VirE2's intracellular trafficking *in planta* has been progressively elucidated recently, there is no clear clue as how VirE2 is associated with plant actomyosin systems. This project aims at finding plant endogenous counterparts, by conducting a comparative kinetic analysis, with which VirE2 shares the same motility features. Such an analysis may provide useful insights to guide the direction of future studies of VirE2's trafficking.

Constructs for respective plant organelles and VirE2 with different fluorescent tags were firstly prepared. Expression of these constructs in plant epidermal cells was achieved with an agroinfiltration method. With confocal microscopy and analytical software, their trafficking patterns, i.e. velocities and displacement rates, were recorded for further analysis.

Results of this study showed that VirE2 and plant cell organelles showed different velocities. Surprisingly, the motility characteristics of the transmembrane domain of MyoB （MyoB-TM） in this study were similar

to that of VirE2. Therefore, further studies on co-expression and interference between VirE2 and MyoB were conducted to test their relationship.

As for the co-expression experiments, majority of MyoB-TM did not co-localize with VirE2 in this study. Occasionally, some MyoB-TM could co-localize with VirE2. And the co-localization could be confirmed by the 3D reconstruction, which ensured that MyoB-TM and VirE2 indeed co-localized instead of an illusion of projection of different optical layers. In addition, tumorigenesis assay of root segments showed that mutation in MyoB2 remarkably abolished *Agrobacterium*-mediated transformation of Arabidopsis, suggesting that MyoB2 may play a critical role in the transformation, presumably due to its impact on VirE2 trafficking. However, overexpression of DUF593, the putative myosin-interacting domain of MyoB, the motility of VirE2 did not change much. Thus the connection of MyoB with VirE2 remains to be further elucidated.

LIST OF TABLES

LIST OF FIGURES

LIST OF ABBREVIATIONS

T-DNA	transferred DNA
Ti plasmid	tumor inducing plasmid
T4SS	type IV secretion system
vir	*virulenc*e
NPC	nuclear pore complex
NLS	nuclear localization signal
VIP2	VirE2 interacting protein 2
GFP	green fluorescent protein
RFP	red fluorescent protein
ER	endoplasmic reticulum
N. benthamiana	*Nicotiana benthamiana*
A. tumefaciens	*Agrobacterium tumefaciens*
TM	transmembrane
MyoB-TM	MyoB transmembrane proteins
GTDs	globular tail domains

1 INTRODUCTION

1.1 Overview of *Agrobacterium*

1.1.1 Overview

Agrobacterium tumefaciens is a small, aerobic, gram-negative soil bacterium which is able to introduce a piece of foreign genetic material known as T-DNA into a plant's genome (Gelvin 2003). Initially the research *Agrobacterium* was intended to understand the fundamental mechanisms of *Agrobacterium* tumor formation and to shed light on animal tumors. Although this yielded no relationship between the tumors of plants and animals, it introduced a possible revolution in plant engineering.

T-DNA is located on a circular Ti plasmid found in almost all bacterium. The unique ability of *A. tumefaciens* to transfer its DNA to plants has led to *Agrobacterium*-mediated transformation being one of the most frequently used techniques in genetic engineering, not only to transform dicotyledons (Hooykaas 1989; Dutt & Grosser 2010), but also to transform monocotyledons plants such as rice (Komari *et al.* 1998). Furthermore, knowledge of *Agrobacterium* has applied to yeast, animal and human system (Bundock & Hooykaas 1996; Relic *et al.* 1998).

1.1.2 Ti plasmid of *Agrobacterium*

Agrobacterium contains a large plasmid of over 200 kb, which is essential for tumor induction in plant tissues. This large plasmid is called Ti plasmid. Components of the Ti plasmid are crucial to the genetic transformation process in genetic engineering of plants. The foremost component of the Ti plasmid is the T-DNA regions, which flank the DNA segment of interest to be transferred. They are specially expressed in the plant and play a direct role in tumor formation in plant tissues. Another component is *vir* genes which encode effectors of the transformation process and the altered T-DNA in which Crown gall disease (Watson *et al.* 1975; Relic *et al.* 1998) causing genes are replaced by the genes of interest. The genes contained in this region differ according to different *Agrobacterium* biotypes, such as octopine and nopaline.

The average size of T-DNA region range around 25 kb. It lies in between two homologous 25 bp repeats. These repeat sequences are known as the right border and left border, as well as targets of the VirD1/VirD2 endonucleases (Sheng & Citovsky 1996). After excision, with the aid of other *Agrobacterium* Vir proteins, the single stranded T-DNA is then exported from the bacterium into plant. Any DNA placed between the T-DNA right and left borders will be transferred to the host cell and

integrated into the nuclear genome (Howard *et al.* 1992).

As mentioned above, T-DNA contains two types of genes. Firstly, the oncogenic genes which encodes for enzymes involved in the synthesis of auxins and cytokinins which are responsible for tumour formation (Akiyoshi *et al.* 1984). Secondly, T-DNA also encodes opines synthesis genes (Kuehnle *et al.* 1991). Opines are synthesized and excreted by the crown gall cells and consumed by *A. tumefaciens* as carbon and nitrogen sources.

Another important region on the Ti plasmid is the 30kb virulence region (*vir* genes). The *vir* region is a regulon organized in six operons that are essential for the T-DNA transfer. The family of *vir* genes includes *virA*, *virB*, *virC*, *virD*, *virG* and *virE* (Hooykaas & Schilperoort 1992; Zupan & Zambryski 1995; Jeon *et al.* 1998). Vir proteins are involved in almost every step of the transformation process from signal recognition, transcriptional activation to the eventual T-DNA integration into the plant nuclear genome (Gelvin 2003).

1.2 Molecular basis of *Agrobacterium* T-DNA transfer

T-DNA transfer and integration into plant cells required not only the joint cooperation of *Agrobacterium* chromosomal and virulence genes (Pitzschke & Hirt 2010), but also the involvement of plant gene products, as shown in a report that a mutant of *Arabidopsis* was resistant to T-DNA transfer by *Agrobacterium* (Mysore *et al.* 2000). When conditions are suitable for injection, such as moisture and the wounding of plant cells, *Agrobacterium* initiates the injection process by chemotaxi and attachment to plant cells. Following signal sensing, virulence gene expression, T-complex formation, and transport apparatus assembly, the T-complex is transferred into the cytoplasm of plant cells. Then the T-DNA is integrated into the chromosome of plant cells after it is absorbed into the plant nucleus. Details on T-DNA transfer are shown in Figure 1-1.

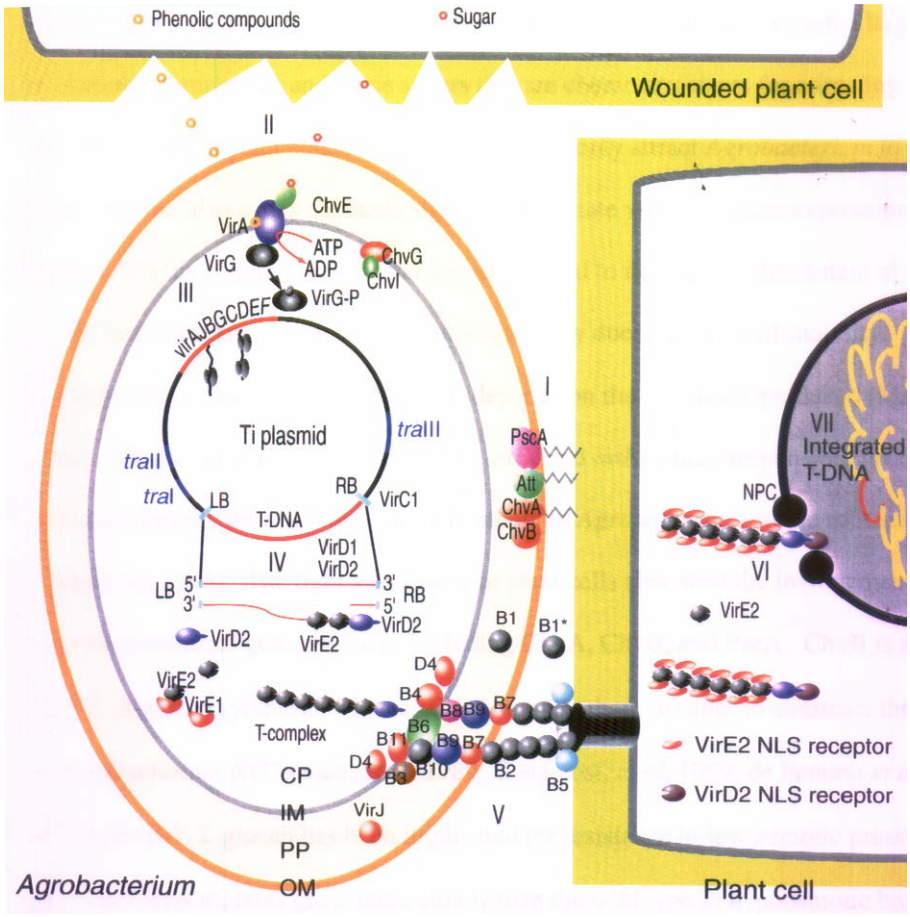

Figure 1- 1 Overview of *Agrobacterium* T-DNA transfer into plant cells.

I, chemotaxi and cell attachment; II, plant signals induction; III, VirA/G activation; IV, T-complex formation; V, T-complex transfer by T4SS; VI, nuclear import of T-DNA/Vir protein complex; VII, T-DNA complex integration into host chromosomes. Abbreviations: CP, cytosolic periplasm; IM, inner membrane; PP, periplasm; OM, outer membrane; LB, left border; RB, right border; NLS, nuclear localization sequence; NPC, nuclear pore complex.

1.2.1 Chemotaxi and cell attachment

The bacterial motility and attachment to plant cells are the early events of *Agrobacterium* infection. They are important since DNA transfer would rarely occur without cell-to-cell contact. The exudates of wounded plant cells contain a large amount of phenolic compounds and some sugars that are chemoattractants for attracting *Agrobacterium* of plant cells. These exudates not only attract *Agrobacterium* to swim to plant cells but also act as chemical signals that initiate virulence gene expression. The motility of *Agrobacterium* is ascribed to its flagella, the mutant of which results in significant reduction in its tumorigenicity due to the loss of moility.

Agrobacterium attachment to plant cells depends on the celluloses produced (Akiyoshi *et al.* 1984). Mutations in genes, like *cel*, *attB*, *attD*, and *attR*, which responsible for cellulose synthesis, heavily decrease the colony numbers of *Agrobacterium* on the root surface. The tight attachment to plant cells also needs the involvement of some other chromosomal gene products, including ChvA, ChvB, and PscA. The mutation of *pscA* alters polysaccharide composition in *Agrobacterium* (Thomashow 1987). ChvB is required for β-1, 3-glucan synthesis, whereas ChvA exports them in order to construct the envelope of *Agrobacterium* (Cangelosi 1989; Iannino 1998). The cyclic β-1, 3-glucan has been implicated for resistance to low osmotic

pressure, and ChvA or ChvB mutants grow more slowly than the wild type in hypoosmotic broth and are avirulent in media of either high or low osmotic pressure (Cangelosi 1990).

1.2.2 Plant signals induction

When plants are wounded, they release a large amount of phenolic compounds for lignin synthesis and some sugars for the repair of cell walls (Winans 1992). *Agrobacterium* senses these small molecules through dimerized VirA (which senses phenolic compounds), and ChvE (which senses sugars) (Shimoda *et al.* 1993). ChvE senses the signals from sugars and passes them to VirA via interaction with VirA in the periplasm. After VirA receives the signals from ChvE and/or that from phenolic compounds through its amino terminus, VirA passes down the signals to VirG, which in turn activates the expression of virulence genes. Apart from the signal compounds from plant cells, VirA-VirG regulation system also needs some environmental factors such as low pH (< 6.0) for virulence gene regulation and expression.

1.2.3 VirA/G activation

The amino terminal domain of VirA can be bound by phenolic compounds secreted by plant cells, while another terminus functions as a kinase to

transfer phosphate to VirG, whose conformation is changed to enable it to bind to some similar sequences, called the *vir* box located upstream of each *vir* promoter, and start the transcription of these genes (Steck *et al.* 1988). Although all the virulence genes including *virA* and *virG* are regulated under the VirA-VirG two-component signal system, some virulence genes appear to be responsive to additional regulatory factors. VirA is normally expressed even without induction signals from VirA-VirG. The *virG* promoter is inducible by phosphate starvation and environmental stress including extremely low pH. The products of virulence genes cause the T-DNA to form a T-complex and assemble the T4SS for the T-complex to pass through the envelope of *Agrobacterium*.

1.2.4 T-complex formation

Normally, the T-complex is considered as a collection of one molecule of single stranded T-DNA, a molecule of pilot VirD2, and a large number of coat proteins, VirE2. This complex is transferred through the cell envelope of and *Agrobacterium* enters the cytoplasm of plant cells.

At both ends of T-DNA region in the Ti plasmid, there are two conserved border-repeat sequences, which can be recognized by VirD1 that bind to them. VirD2 functions as a nickase, which can specifically bind to the

border sequences before cutting T-DNA out of the Ti plasmid to generate single-stranded DNA, T-strand. VirD2 then attaches to the 5' end of the T-strand. While the T-strand is extended from the right border to left border, VirE2 immediately binds to the ssDNA to protect it from degradation (Grange *et al.* 2008). In the octopine-type of *Agrobacterium*, VirC1 can bind to the overdrive sequences near the T-DNA region, and contribute to T-strand formation. Its mutant does not abolish tumorigenicity but attenuates it 100-fold. VirE2 is also found to pass through T4SS alone, unaccompanied by the T-complex, into the cytoplasm of plant cells with the help, binding, and protection from its chaperone, VirE1 (Sundberg & Ream 1999). Besides, the T-complex and VirE2 can also be secreted into the plant periplasm independently (Gelvin 1998).

1.2.5 T-complex transfer by T4SS

The VirB channel that is found in *Agrobacterium* and which transfers the T-complex into plant cells is classified as a Type IV secretion channel. Well characterized Type IV channels include the 1) VirB channel in *Agrobacterium*, 2) Ptl channel in *Bordetella pertussis* to secrete proteins, namely, pertussis toxin, across bacterial membrane, 3) Tra system of IncN plasmid pKM101, and the 4) plasmid conjugal transfer system of RP4 (Burns 1999). Almost every component of the VirB channel has its

corresponding elements in the other three Type IV secretion systems (Winans *et al.* 1996). With the full expression of *vir* genes, *Agrobacterium* strains also transfer the IncQ plasmid, RSF1010, into plant cells or between *Agrobacterium* like F plasmid conjugation systems (Bohne *et al.* 1998; Stahl *et al.* 1998).

1.2.6 Nuclear import of T-DNA/Vir protein complex

In order to integrate T-DNA into the chromosome of plants after the T-complex is transferred, the T-complex must be further transported into the nuclei of plant cells. Generally, molecular transport across the nuclear envelope involves the NPC, a structure of around 125,000 kDa. This transport is bi-directional and occurs exclusively through the NPC. The NPC can allow small molecules (up to 40 kDa) to passively diffuse in and out through it. Large molecules, however, are mediated by a specific NLS within the transported molecules (Conti *et al.* 1998; Zhu *et al.* 2015). The T-complex is a large structure, which is estimated to be about 3.6 μm in diameter with a molecular weight of around 5×10^7 Daltons. Therefore, it is definitely impossible for the T-complex to diffuse into plant nuclei. Like some coat proteins of enveloped viruses, VirD2 and VirE2 both have NLSs, which guide the T-complex through the pore to plant nuclei (Howard *et al.* 1992; Ream 1998a). VirD2 possesses two NLSs and VirE2 has one NLS. A

mutation in any one of the NLS domains in VirD2 and VirE2 attenuates the tumorrigenicity but does not fully disable it. This indicates that all three NLSs cooperate together in the transmission of the T-complex into plant nuclei.

1.2.7 T-DNA complex integration into host chromosomes

T-DNA integration is the last step before the expression of genes within T-DNA. As for the nuclear localization process of the T-complex, the details of T-DNA integration are not clear. However, it is proven that the mechanisms of integrating the left and right border of T-DNA into plant DNA are different. The right border of T-DNA attached to VirD2 is always exactly be integrated into the plant DNA without the loss of any nucleotides. The integration of the left border, however, results in the loss of hundreds of base pairs (Mayerhofer *et al.* 1991). VirD2 not only guides the T-complex into plant cells, but also protects the 5' end from nuclease attack and ligates the 5' end of T-strand (Jasper & Steinbiss 1994)into the plant DNA. The complex of VirD3-DNA is also proven to have ligation ability, since approximately half of oligonucleotide substrates are cleaved and ligated by VirD2. This is further supported by observation that an increase in the amount of VirD2 or reactions incubation for protracted periods neither increases nor decreased the equilibrium between nicked and intact

molecules (Jasper & Steinbiss 1994). To detect T-DNA transfer into the nuclei of plant cells even without the integration of the T-strand and expression of the genes associated with T-DNA, previous study (Gardner & Knauf 1986) has proven that T-DNA can be transferred into plant cells and integrated into plant nuclei in an unstable manner. Another study (Ream 1998b) also considers that VirF may involve T-DNA integration since it is secreted into plant cells through the T-complex transport apparatus inappropriately and it does not contribute the transport of the T-complex into the nuclei of plants. Basically, most think that the integration of T-DNA involves the gene products of *Agrobacterium* and is also aided by plant cell proteins. Once T-DNA is integrated into plant DNA, it will not move around in the genome of plants.

2 LITERATURE REVIEW

2.1 Functions of VirE2

The T-DNA complex contains only one 5'end covalently attached VirD2 protein. However, it is coated by at least 600 VirE2 molecules (Citovsky *et al.* 1992). This highlights that VirE2 is significantly the most abundant when compared to other Vir proteins. Besides, VirE2 is known to perform an unusually big number of functions (Ward & Zambryski 2001).

VirE2 possesses six main explored functions (Ward & Zambryski 2001). Firstly, VirE2 coats the T-strand, maintaining its conformation and protecting it from degradation. Secondly, VirE2 associates with VirE1 which is needed for its export. Thirdly, VirE2 independently exits as part of the T complex or *Agrobacterium* via the type IV secretion system. Fourthly, VirE2 forms a pore facilitating cargoes for transport. In addition, VirD2 and VirE2 interact with plant chaperones and other factors which may target the T-complex to the nucleus. Lastly, VirE2 interacts with factors such as VIP2. This promotes interaction with chromatin and facilitates integration of the T-strand into the nuclear genome. All the above has prompted scientist to carry out research on VirE2. Understanding VirE2 will shed light on the intracellular trafficking of a foreign protein within the host cell and

eventually that of T-DNA trafficking.

2.2 Organelle movements in plant cells

Organelles in plant cells possess high motilities, the speed values of which range from 3 to 7 μm/sec and 20 to 60 μm/sec for land plants and characean algal cells, respectively. Moreover, their movements are essential for the distribution of matrix in plant cells. It is generally accepted that actin cytoskeleton and its motor proteins, the myosin family, propel organelle motilities (Turkina & Sokolov 2001). Myosin VIII, as well as myosin XI, is considered as the main class expressed in most plants. Myosin VIII has been proved to be a slow motor protein, while myosin XI is considered as the fastest motor protein to date. In addition, most organelle movements are regulated by motor proteins from class of myosin XI. However, it is not so clear how the motor proteins bind plant cell organelles (Buchnik *et al.* 2015).

Immunohistochemical methods are used to first predicate the relation between plant myosins and different organelles (Tang *et al.* 1989; Liu *et al.* 2001; Yokota *et al.* 2009). Later, fluorescent methods are used to fuse with various myosins, which further confirm the findings above. Previous study

(Li & Nebenführ 2007) proved that fluorescence tagged myosin XI-1 and XI-2 proteins mainly co-localized peroxisomes and occasionally with Golgi stacks. Another study (Sattarzadeh 2013) demonstrated that most fragments from different myosin XI families successfully co-localized to Golgi stacks and mitochondria, however only that from myosin XI-F co-localized to peroxisomes. Strangely, the GFP fused with full-length myosin XI-K showed no obvious co-localization with any plant cell organelles. Latest studies (Peremyslov *et al*. 2012; Peremyslov *et al.* 2013) indicated that GFP with full-length myosin XI-K only partially co-localized with ER and very seldom with Golgi stacks. Therefore, it remains to be verified how myosins attach to Golgi stacks, mitochondria and peroxisomes.

An earlier study (Avisar *et al.* 2008) also showed that the overexpression of myosin XI proteins inhibited the movements of Golgi stacks, mitochondria and peroxisomes. This indicated that plant cell organelle trafficking is myosin-dependent. Interestingly, a research group (Peremyslov *et al.* 2013) screened a family of myosin receptors called MyoB, and they hypothesized that MyoB may bind myosin XI-K to form a new transport vesicle. This vesicle allows cargoes in plant cells to attach and move along with myosin XI-K. This model deserves more research for it is novel, specific and makes sense.

2.3 Aims of the project

Previous studies have revealed that the trafficking of VirE2 is F-actin associated and driven by myosins, in the same manner as that of plant cell organelles. Phenotypic observations of VirE2's intracellular trafficking have been documented recently (unpublished data). However, the mechanism that allows VirE2's utilization of such an actomyosin motility system remains unclear. This project aims at finding the endogenous counterparts that share the same motility features with VirE2, so that provide valuable clues for elucidating how VirE2 achieves its intracellular trafficking.

3 MATERIALS AND METHODS

In this study, the trafficking of plant cell organelles in epidermal cells of *N. benthamiana* leaf were visualized firstly with RFP targeted plant cell organelles expressed in *N. benthamiana* plants. The trafficking patterns of RFP targeted organelles and VirE2 signals were tracked with spinning disc confocal microscopy. Secondly, the TM domains of MyoB1 and MyoB2 were cloned to label MyoB decorated vesicles. A kinetic comparison between the motility of MyoB decorated vesicles and that of VirE2 was conducted. Thirdly, to determine whether there is co-expression of MyoB-TM and VirE2 in plant cells, *Agrobacterium tumefaciens* containing GFP tagged VirE2 and that containing mCherry tagged MyoB-TM were evenly mixed and an agroinfiltration assay was conducted by using *Nicotiana benthamiana* leaf as the host. Confocal microscopy was used to visualize the fluorescence signals. Lastly, to test the involvement of MyoB in *Agrobacterium*-mediated transformation, a strategy in genetic perspective was employed. Insertional mutants of Arabidopsis *myoB1* and *myoB2* were purchased from ABRC. Homozygous seeds were PCR-confirmed prior to germination. 10-day-old seedlings on MS agar plates were collected and their roots were cut into approximately 5 mm segments. These root segments were agroinfected with tumor inducing strain A348.

3.1 Media and solutions

Table 3-1 listed media and solutions used in this study. All reagents used are commercial products. Before culturing, the media and solutions should be sterilized to eliminate the interference of microbial contamination.

Table 3- 1 Media and solutions used in this study

Medium/Solution	Recipe	Reference
MG/L	500 ml LB, 10 g mannitol, 2.32 g sodium glutamate, 0.5 g KH_2PO_4, 0.2 g NaCl, 0.2 g $MgSO_4 \cdot 7H_2O$, 2 μg biotin, pH=7.0	Cangelosi *et al.* 1991
LB Broth	10 g Peptone 140, 5 g Yeast Extract, 10 g Sodium Chloride	Bertani 1951
Agroinfiltration Buffer	10 mM MES, 10 mM $MgCl_2$, PH=5.5	Li *et al.* 2013

3.2 Bacterial strains and culture conditions

Table 3-2 listed bacterial strains used in this study. *A. tumefaciens* was cultured in MG/L at 28°C, and *E. coli* was cultured in Luria-Bertani (LB) broth at 37°C, both in a 200 rpm orbital shaker.

Table 3- 2 Strains used in this study

Strains	Relevant characteristics	Source
A. tumefaciens		
EHA105	Wild-type, agropine strain containing pTiBo542, disarmed	Bertani 1951
EHA105 *virE2*	EHA105, *virE2* mutant strain with CDS knockout	Li *et al.* 2013
VES11	EHA105, *virE2* fused with GFP11 at +162	Li *et al.* 2013
Escherichia coli		
DH5α		

3.3 Constructs

Table 3-3 listed plasmids used in this study. Different primers were used to deal with vectors and get inserts. Constructs obtained here were stored in -80℃ with glycerol before utilization.

Table 3- 3 Plasmids used in this study

Plasmids	Relevant characteristics	Source
pQH121M	Modified version pBI121, with *GusA* replaced by MCS.	Li *et al.* 2013
pQH121M-MC	pQH121M inserted with the CDS of mCherry down stream of *mas* promoter.	This study
pQH121M-TM1-MC	pQH121M-MC with MyoB1 -TM inserted at SalI - BamH1 down stream of *mas* promoter.	This study
pQH121M-TM3-MC	pQH121M-MC with MyoB2 -TM inserted at SalI - BamH1 down stream of *mas* promoter.	This study
pQH121M-DUF1-MC	pQH121M-MC with MyoB1 -DUF593 inserted at SalI - BamH1 down stream of *mas* promoter.	This study
pQH121M-DUF3-MC	pQH121M-MC with MyoB2 -DUF593 inserted at SalI - BamH1 down stream of *mas* promoter.	This study

Figure 3-1 showed the schematic diagram of constructs used in this study, representing pQH121M-TM-MC and pQH121M-DUF-MC, in line with Table 3-3.

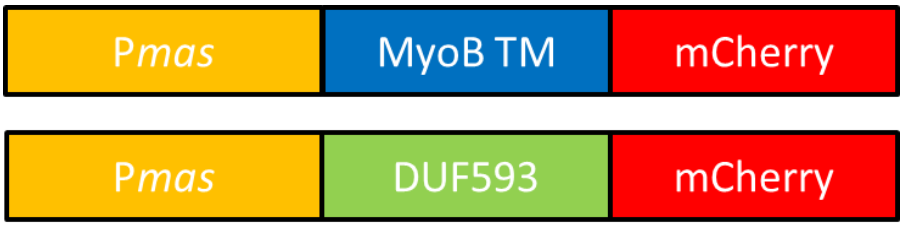

Figure 3- 1 Schematic diagram of constructs used in this study.

Top row, pQH121M-TM-MC. Bottom row, pQH121M-DUF-MC

3.4 Plant species

Table 3-4 listed plant species used in this study. Nb307A with a big fragment GFP1-10 was used for infiltration and construct expression. Nb307A was cultured under artificial light with fertilizer.

Table 3- 4 Plant species used in this study

Plant	Description
Nicotiana benthamiana	
Nb307A	Transgenic *N. benthamiana* plants with a big fragment GFP1-10 was constitutively expressed

3.5 Agroinfiltration

Agrobacteria culture (2 ml) was grown overnight with appropriate antibiotics, and further cultured with 1:50 dilution for additional 6~7 hours until OD_{600} reaches 1. The bacteria cells were pelleted by centrifuging 3 minutes at 4000 g, and then resuspended in 10 ml infiltration buffer (10 mM $MgCl_2$, 10 mM MES, PH=5.5), OD_{600}≈0.3-0.4. This bacteria suspension was then placed in a syringe, without a needle. The tip of the syringe was pressed against the abaxial side (lower side) of a fully expanded leaf from a 6-8 weeks old *Nicotiana benthamiana*, while applying gentle counter-pressure to the other side with an index finger. The bacteria suspension was then push-injected into the airspaces inside the leaf through stomata, or through tiny incisions caused by the syringe tip. Transient expression can be optimally visualized 2 days after infiltration.

3.6 Confocal Microscopy and Analysis

A PerkinElmer UltraView Vox Spinning Disk system with EM-CCD cameras was used for confocal microscopy. Agroinfiltrated leaf tissues were detached from *N. benthamiana* plants to observe leaf epidermis and put in 2% low-melting agarose gel on a glass slide with a coverslip. All images were taken in multiple focal planes (Z-stacks), and were processed to show

the extended focus image, or 3D opacity view by Volocity® 3D Image Analysis Software 6.2.1.

Dynamics of VirE2 and other organelles signals were manually tracked using Velocity software, with at least 20 tracks for each sample. Trafficking paths were shown by joining origins together in a centralized chart. Mean velocity was determined by averaging the velocity of the paths obtained by the software.

3.7 Visualization of *Agrobacterium*-delivered VirE2 protein *in planta*

Visualization of bacterium-originated VirE2 was achieved by a split GFP approach, which was fully described by Li *et al.*, 2013. Briefly, VirE2 was tagged with a small GFP fragment GFP11 at a reported permissive site. A big fragment GFP1-10 was expressed in recipient cells. Upon delivery of VirE3-GFP11 by agrobacteria, GFP1-10 binds to GFP11, forming VirE3-GFP_{comp}, and fluorescence is restored (Li *et al.* 2013). Details on the split GFP approach are shown in Figure 3-2.

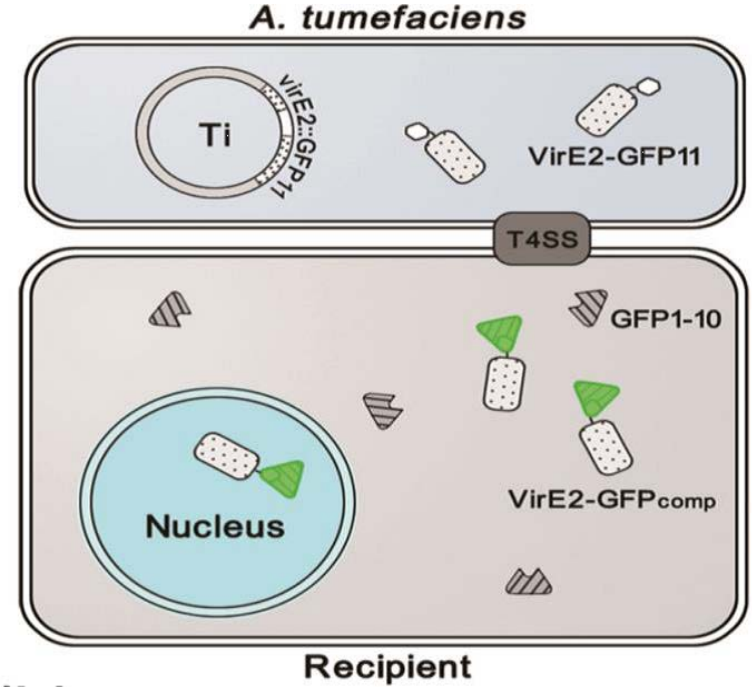

Figure 3- 2 Schematic representation of a split-GFP approach of visualizing bacterium-delivered VirE2 in recipient cells

4 RESULTS

4.1 Plant cell organelles and VirE2 intracellular trafficking

Different plant cell organelles possess different motilities, and their motions are easily influenced by lots of factors including environment temperatures, the growth stages of plant, and the positons of investigated leaves in plant. As for VirE2, an exogenous protein for plant cells, it possesses its own trafficking mode highly related to plant cells, which is similar to that of plant cell organelles. Therefore it makes sense to study the co-relation between the movement of VirE2 in plant cells and that of plant cell organelles.

To compare the trafficking difference of VirE2 and plant cell organelles, and further conduct a comparative kinetic analysis of VirE2 intracellular trafficking, the movements of different fluorescence tagged plant cell organelles and VirE2 were tracked and their mean velocities were calculated as well in this study.

4.1.1 Trafficking of plant cell organelles and VirE2

To visualize the trafficking of plant cell organelles in epidermal cells of *N. benthamiana* leaf, RFP targeted plant cell organelles were expressed in *N.*

benthamiana plants. The trafficking patterns of RFP targeted organelles and VirE2 signals were tracked with spinning disc confocal microscopy. More than 20 Golgi stacks were tracked to reflect the trafficking patterns. Volocity software was employed for further determination of their velocities, including mean velocity and displacement rate, and trafficking patterns.

As shown in Figure 4-1A, RFP targeted Golgi stacks were successfully expressed and tracked under confocal microscopy. It deserved to be mentioned that most of the cells within the infiltrated area expressed the RFP marker. Presented as red dots in Figure 4-1A, RFP targeted Golgi stacks were full of view. Majority of the red dots were distributed along the membrane skeleton of plant cells.

In plant cells, mitochondria act as an important organelle to produce ATP to power the metabolic process. As the powerhouses of plant cells, mitochondria play an important role in cells' aerobic respiration (Millar 2014). In this study, the presented feature of mitochondria was similar to that of Golgi stacks, both of which were red dots (Figure 4-1A). Different with Golgi stacks, RFP targeted mitochondria were countable in this study. And the motility of mitochondria was weaker than that of Golgi stacks

(Figure 4-1B). No obvious movement of mitochondria was detected. This may be related to the fact that mitochondria function as the producer of power for plant cells activity. Therefore it is unnecessary for mitochondria in plant cells to move. As a supplement, either ATP produced by mitochondria are distributed to everywhere inside the cell with the movement of cytoplasm, or others organelles move toward mitochondria to trap ATP.

Peroxisomes own many different functions on metabolic process of living plant cells. Based on cell type, environmental conditions and the species, they differ in abundance and size (Jedd & Chua 2002; Zhang & Hu 2009). In this study, RFP targeted peroxisomes were successfully expressed and tracked under confocal microscopy according to Figure 4-1. Presented as red dots as well, RFP targeted peroxisomes are in different sizes and spread along microfilaments (Jedd & Chua 2002). Moreover, in some part of plant cell, peroxisomes tended to aggregate together according to Figure 4-1A. This may be because that this part of plant cell was in larger demand of peroxisomes. Consistent with Golgi stacks, peroxisomes exhibit obvious directional movement according to Figure 4-1B, which is in line with previous study (Jedd & Chua 2002).

Plastid is a unique organelle of plant cells, which is considered as one of the differences between plant and animal cells. In plant tissues, it plays an essential role in carbohydrate, amino acid, lipid and secondary metabolism (Kessler & Schnell 2006). Similar to the visualization of the trafficking of other organelles in plant cells, the trafficking of plastid was analyzed in this study. The size of RFP targeted plastids was larger than that of other organelles in this study. Furthermore, similar to mitochondria, plastids in Figure 4-1A was also countable. However, the motility of plastids was the weakest among all of the organelles as shown in Figure 4-1B. Almost no movement of plastids was detected. This may be due to the fact that plastids are the houses for photosynthesis. In addition, the size of plastid is huge. Therefore it is hard and needless for plastid to move everywhere.

VirE2 belongs to the Vir proteins family. It has six different functions (Ward & Zambryski 2001), which are essential for genetic transformation by *Agrobacterium tumefaciens*. To analyze the relationship between the movement of VirE2 and that of plant cell organelles, GFP tagged VirE2 was constructed as described previously (Li *et al.* 2013). As a result, bacterium-delivered VirE2 were successfully observed under confocal microscopy as shown in the last image of Figure 4-1A. Different with the features of plant cell organelles, VirE2 showed a unique feature in this

study. VirE2 presented different morphologies in the same cell, including dot, strip, stick and string. The distribution of VirE2 is relatively homogeneous in view of Figure 4-1A. The trafficking patterns of VirE2 were shown in Figure 4-1B. A divergent distribution was put up through Figure 4-1B. There is no obvious form of motion as well. However, a published paper (Li *et al.* 2013) described that most of VirE2 in their study tended to move in a nearly liner direction. This difference may be caused by the different conditions of environment and plant.

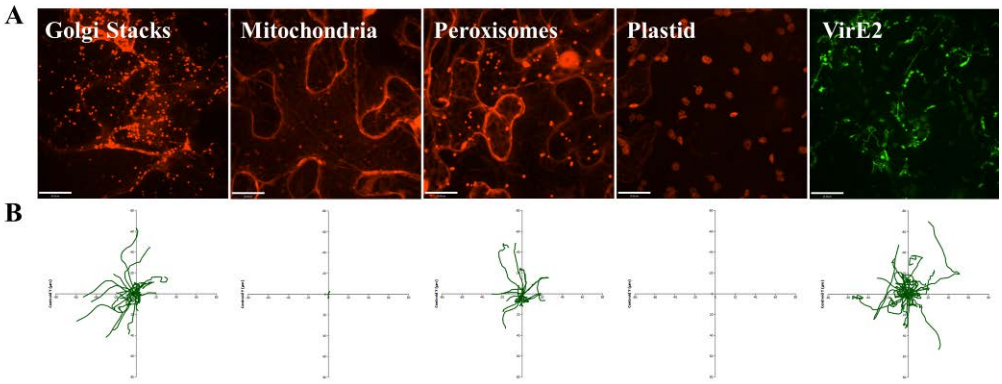

Figure 4- 1Trafficking comparison between plant cell organelles and VirE2.

(A) Images of plant cell organelles and VirE2 by confocal microscopy. (B) Trafficking patterns of plant cell organelles and VirE2 by Volocity software.

4.1.2 Velocity and displacement rate of plant cell organelles and VirE2

Mean velocity and displacement rate of plant cell organelles and VirE2 are shown in Table 4-1. According to Table 4-1, the mean velocity of Golgi stacks reached 0.889 μm/sec, while the mean displacement rate of Golgi stacks was 0.611 μm/sec. Different Golgi stacks had different velocities ranged between 0.167 μm/sec and 2.540 μm/sec, while the displacement rates ranged between 0.055 μm/sec and 2.440 μm/sec. Different velocities and displacement rates satisfied the requirements that plant cells tend to transfer different Golgi stacks to different area inside by membrane skeleton.

For mitochondria, in line with the result in Figure 4-1B, the mean velocity was just 0.025 μm/sec, while the mean displacement rate of mitochondria was 0.014 μm/sec. Mitochondria in this study moved with a velocity range from 0.008 μm/sec to 0.090 μm/sec, while the displacement rates ranged from 0.004 μm/sec to 0.055 μm/sec. Data in Table 4-2 further indicated that mitochondria showed poor motility in plant cells.

In this study, the mean velocity of peroxisomes reached 0.285 μm/sec according to Table 4-1, while the mean displacement rate was 0.155 μm/sec. The peak velocity was 0.891 μm/sec, while the peak displacement rate was

0.354 μm/sec. Results in this study were quite different with that in previous study (Avisar *et al.* 2008). This may be because that the movement of peroxisomes could be affected by many factors such as environment conditions and cell types.

In line with the result in Figure 4-1B for plastid, both the mean velocity and the mean displacement rate of plastid was near 0, which indicated that, in plant cells, plastids exhibited no motility.

Further results on mean velocity and displacement rate of VirE2 were also shown in Table 4-1. The mean velocity of VirE2 was 0.433 μm/sec, while the mean displacement rate of was 0.166 μm/sec according to Table 4-1. VirE2 in this study moved at a speed of 0.086~0.991 μm/sec, while that in previous study was 1.3~3.1 μm/sec (Li *et al.* 2013). Reasons for the huge difference are complicated. Except the conditions of environment and plant, sizes may also be an important factor (Li *et al.* 2013).

Table 4- 1 Velocities and displacement rates of plant cell organelles and VirE2

	Parameters	Highest value (μm/sec)	Lowest value (μm/sec)	Mean value (μm/sec)
Golgi stacks	**Velocity**	2.540	0.167	0.889
	Displacement rate	2.440	0.055	0.611
Mitochondria	**Velocity**	0.090	0.008	0.025
	Displacement rate	0.055	0.004	0.014
Peroxisomes	**Velocity**	0.891	0.052	0.285
	Displacement rate	0.354	0.039	0.155
Plastid	**Velocity**	0	0	0
	Displacement rate	0	0	0
VirE2	**Velocity**	0.991	0.086	0.433
	Displacement rate	0.535	0.016	0.166

Figure 4-2 summarized the mean velocities of different plant cell organelles and VirE2. The samples used were taken from *Nicotiana benthamiana* leaves cultured in the same situation.

According to Figure 4-2, different organelles owned different motilities. No obvious relation between the movement of VirE2 and that of plant cell organelles was discovered in this study.

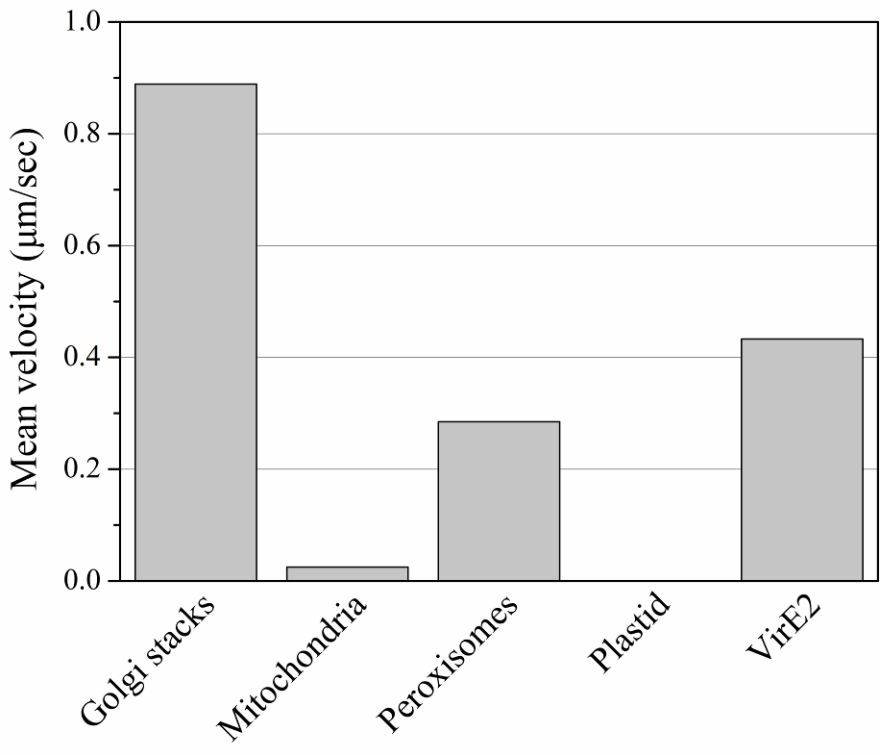

Figure 4- 2 Mean velocity comparison between plant cell organelles and VirE2.

4.2 Biological analysis and intracellular trafficking of MyoB proteins

MyoB1 and MyoB2 are transmembrane proteins characterized recently (Peremyslov *et al.* 2013). These two MyoB proteins act as membrane-anchored core myosin receptors, and this function is mainly realized by the conserved TM and DUF593 domains in MyoB proteins. Moreover, this group (Peremyslov *et al.* 2013) proved that the TM domains of MyoB can bind to a distinct type of motile cargos. The nature of such cargoes remains to be determined. Taken that VirE2 is predominantly driven by myosins, the MyoB decorated vesicles may have to do with VirE2's motility. In this study, the TM domains of MyoB1 and MyoB2 were cloned to label MyoB decorated vesicles. A kinetic comparison between the motility of MyoB decorated vesicles and that of VirE2 was conducted.

4.2.1 Biological analysis and trafficking of MyoB-TM

To analyze the localization of MyoB-TM in plant cells, constructs containing GFP tagged endoplasmic reticulum were evenly mixed with that containing mCherry tagged MyoB-TM. Then the mixture was infiltrated in epidermal cells of *Nicotiana benthamiana* leaf to visualize the signals. Confocal microscopy was used as well.

Figure 4-3 showed the localization of MyoB-TM in *Nicotiana benthamiana* epidermal cells. Figure 4-3A represented the localization of MyoB1-TM. It is obvious that, in plant cells, mCherry tagged MyoB1-TM localized to GFP tagged endoplasmic reticulum. Similar with MyoB1-TM, mCherry tagged MyoB3-TM also tended to localized to GFP tagged endoplasmic reticulum, as shown in Figure 4-3B.

Both MyoB-TM displayed similar motion mode. And both of them tend to move along endoplasmic reticulum. Figure 4-4 showed the movement of MyoB1-TM in endoplasmic reticulum. From 1 to 5, the solid arrows marked the movement of one MyoB1-TM. It was easily observed that MyoB1-TM moved along GFP tagged endoplasmic reticulum in plant cells.

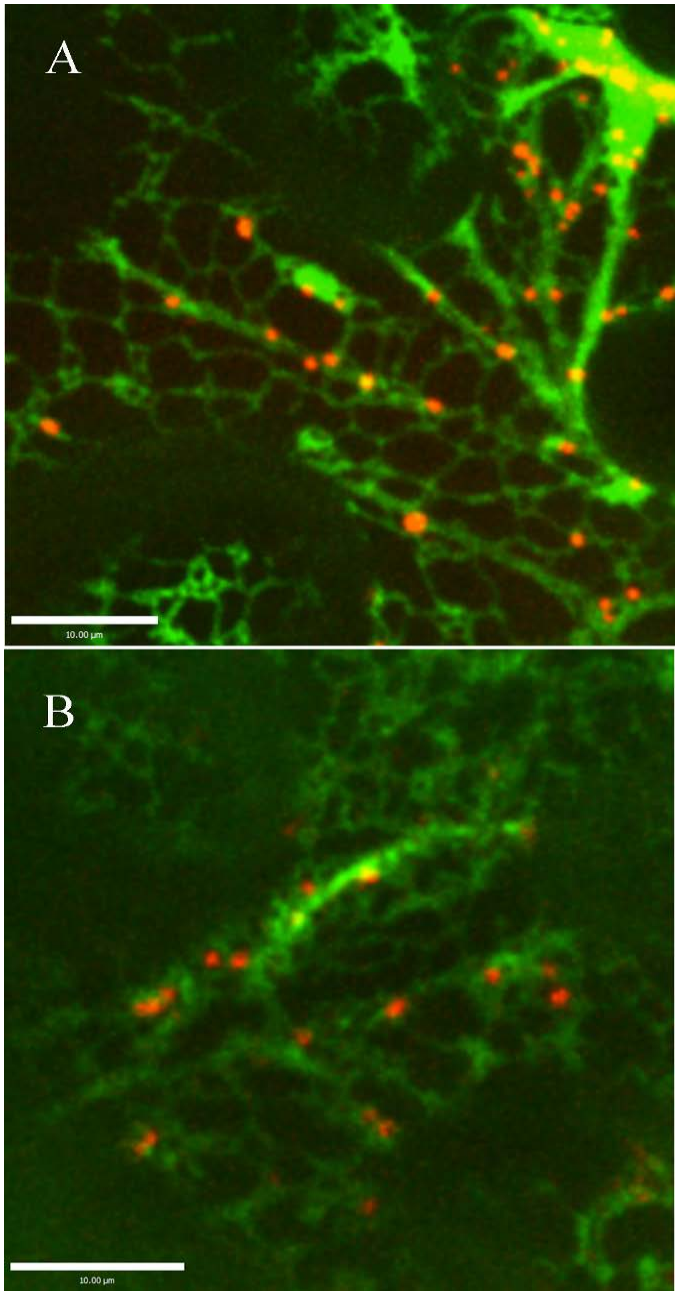

Figure 4- 3 Localization of MyoB-TM in plant cells.

Green, ER marker; Red, (A) MyoB1-TM. (B) MyoB3-TM.

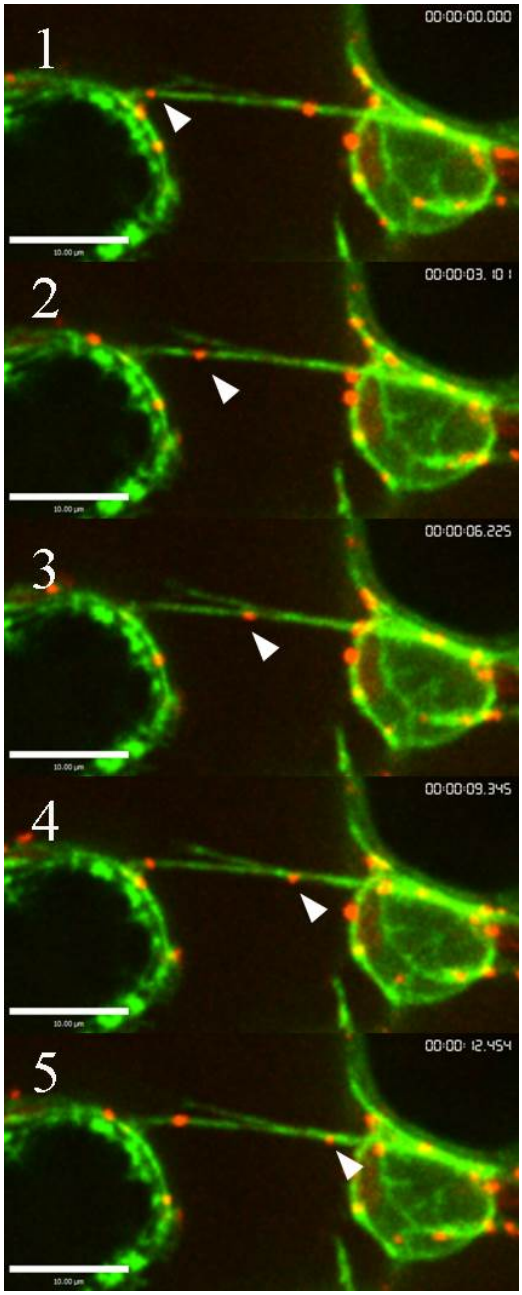

Figure 4- 4 Movement of MyoB1-TM along endoplasmic reticulum

Previous study (Peremyslov *et al.* 2013) has proved that the DUF593 domain of MyoB could bind the GTD domain of Myosin XI. Thus MyoB could be considered as one of myosin receptors. Furthermore, MyoB decorated vesicles can act as a transport vehicle. Moreover, Myosin XI was proved to move along actin filament in plant cells. Therefore cargos transported by MyoB-myosin system could theoretically move along actin filament with a fast speed. Similar to the visualization of the trafficking of organelles and VirE2 in epidermal cells of *Nicotiana benthamiana* leaf, confocal microscopy and velocity software were used to analysis the movement, velocities and trafficking patterns of MyoB-TM (Figure 4-5 and Table 4-2).

The left column of Figure 4-5 showed the feature and trafficking pattern of mCherry tagged MyoB1-TM. Under confocal microscopy, the presented feature of mCherry tagged MyoB1-TM was similar to that of most organelles in plant cells, all of which were red dots-like balls, according to Figure 4-5A. The trafficking patterns of mCherry tagged MyoB1-TM were shown in the left column of Figure 4-5B. More than 20 MyoB1-TM were tracked for the trafficking patterns. As expected, mCherry tagged MyoB1-TM showed great motility as well as VirE2, the right column of

Figure 4-5. Interestingly, the motion of mCherry tagged MyoB1-TM showed prominent directionality, when compared with VirE2. This indicated that MyoB1-TM may prefer to transport specific cargos to particular locations in plant cell.

The middle column of Figure 4-5 showed the feature and trafficking pattern of mCherry tagged MyoB3-TM. As shown in Figure 4-5A, MyoB3-TM were dot-like balls with different size. The huge ones may be formed by the aggregation of mini ones. The trafficking patterns of mCherry tagged MyoB3-TM were shown in the middle column of Figure 4-5B. Same as MyoB1-TM, more than 20 MyoB3-TM were tracked for the trafficking patterns. And mCherry tagged MyoB3-TM also showed great motility as well as MyoB1-TM and VirE2. Different with MyoB1-TM, but similar to VirE2, the motion of mCherry tagged MyoB3-TM did not show clear directionality. This indicated that MyoB3-TM may act as universal cargo transport vesicles in plant cell.

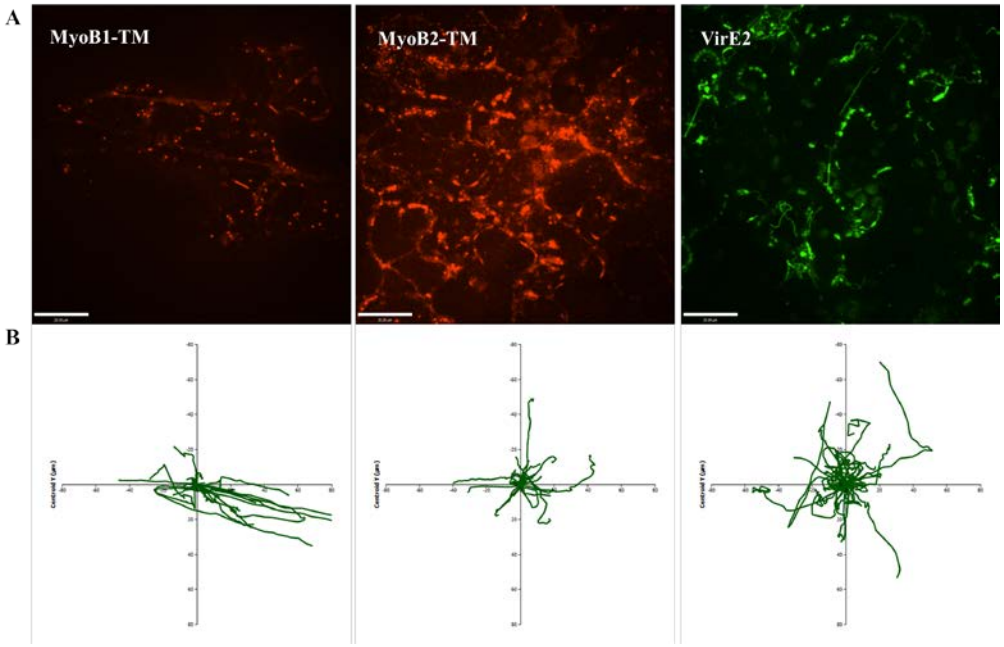

Figure 4- 5 Images and trafficking patterns of MyoB-TM and VirE2.

(A) Images of MyoB-TM and VirE2 by confocal microscopy. (B) Trafficking patterns of MyoB-TM and VirE2 by Volocity software.

Table 4-2 showed the mean velocity and displacement rate of MyoB1-TM. The mean velocity of MyoB1-TM reached 0.524 μm/sec according to Table 4-2, while the mean displacement rate of MyoB1-TM was 0.345 μm/sec. MyoB1-TM in this study moved with a velocity ranged from 0.072 μm/sec to 2.360 μm/sec, while the displacement rates ranged from 0.042 μm/sec to 2.330 μm/sec.

The mean velocity of MyoB3-TM was 0.389 μm/sec, which was less than that of MyoB1-TM. The mean displacement rate of MyoB3-TM was 0.288 μm/sec. MyoB3-TM in this study moved with a velocity ranged from 0.034 μm/sec to 1.740 μm/sec, while the displacement rates ranged from 0.031 μm/sec to 1.640 μm/sec.

Table 4- 2 Velocities and displacement rates of MyoB-TM

	Parameters	Highest value (μm/sec)	Lowest value (μm/sec)	Mean value (μm/sec)
MyoB1-TM	**Velocity**	2.360	0.072	0.524
	Displacement rate	2.330	0.042	0.345
MyoB3-TM	**Velocity**	1.740	0.034	0.389
	Displacement rate	1.640	0.031	0.288

Figure 4-6 summarized the mean velocities of MyoB-TM and VirE2 recorded in this study. An obvious result that the mean velocity of VirE2 (0.433 μm/sec) is between that of MyoB1-TM (0.524 μm/sec) and MyoB3-TM (0.389 μm/sec). They showed almost same mean velocity as shown in Figure 4-6.

Based on both the feature of mean velocities owned by VirE2, MyoB1-TM and MyoB3-TM, and the fact that VirE2 tends to move along actin filament, a hypothesis that the movement of VirE2 may be connected with that of MyoB1-TM and/or MyoB3-TM was put up in this study. In other words, VirE2 were supposed to be the cargos of MyoB1-TM and/or MyoB3-TM. Further biological assays to verify this hypothesis, including co-expression of MyoB-TM and VirE2, interfering VirE2 by overexpressing DUF593, and root tumorigenesis of MyoB mutant plants were conducted.

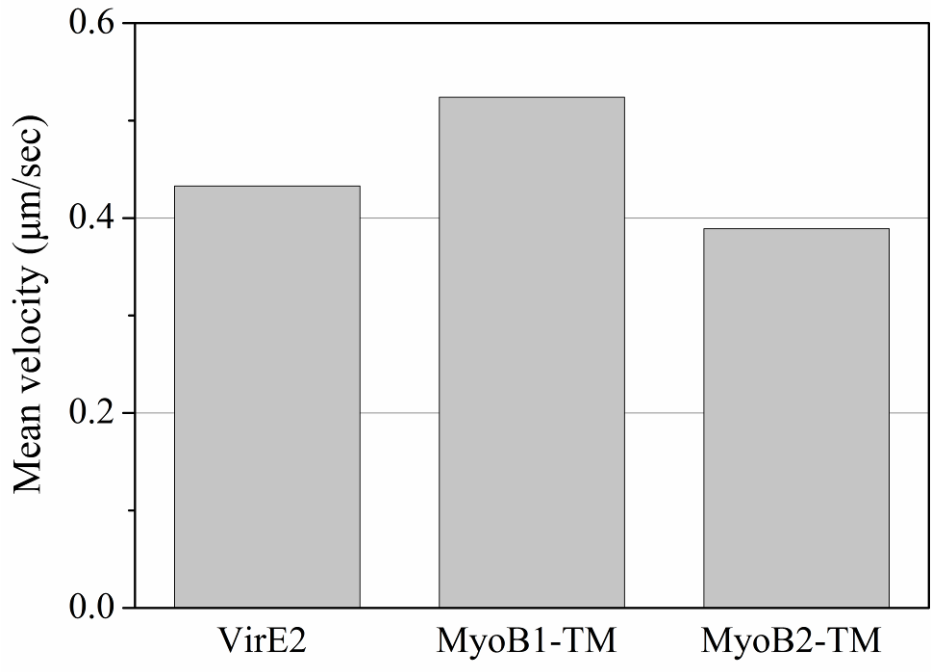

Figure 4- 6 Mean velocities of VirE2 and MyoB transmembrane proteins

4.3 Biological analysis of the relation between MyoB and VirE2

4.3.1 Co-expression of MyoB-TM and VirE2

To determine whether there is co-expression of MyoB-TM and VirE2 in plant cells, *Agrobacterium tumefaciens* containing GFP tagged VirE2 and that containing mCherry tagged MyoB-TM were evenly mixed first. Then an agroinfiltration assay was conducted by using *Nicotiana benthamiana* leaf as the host. Confocal microscopy was used to visualize the fluorescence signals.

Figure 4-7 showed co-expression of MyoB-TM and VirE2 in plant cells. GFP tagged VirE2 and mCherry tagged MyoB-TM are all successfully expressed as shown in Figure 4-7. Figure 4-7A represented the co-expression of MyoB1-TM and VirE2, from which, little co-localization was observed. Most of VirE2 and MyoB1-TM were clearly separated. Moreover, VirE2 and MyoB1-TM seemed to localize different regions in the same plant cell. The relation between VirE2 and MyoB3-TM was similar to that between VirE2 and MyoB1-TM.

Occasionally, some MyoB-TM could co-localize VirE2. As shown in Figure 4-8, MyoB1-TM successfully co-localized with VirE2. And the 3D reconstruction image further confirmed that, instead of distributing in

different layers, MyoB1-TM indeed co-localized with VirE2.

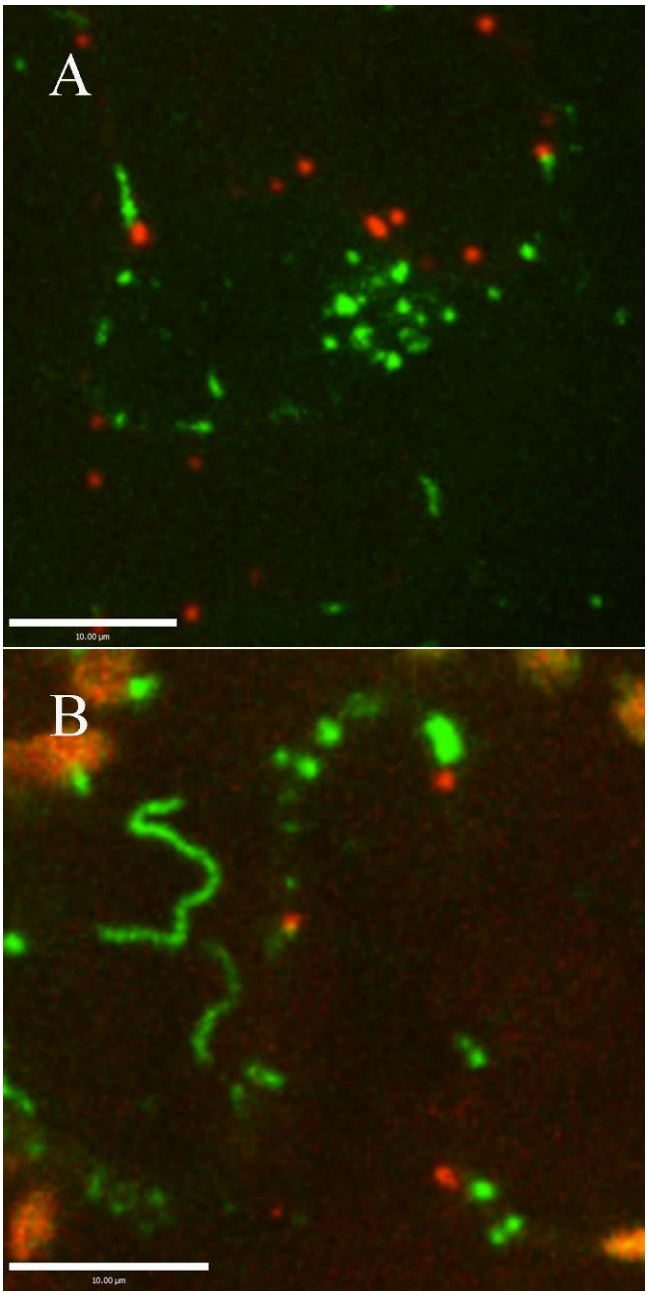

Figure 4- 7 Co-expression of MyoB-TM and VirE2 in plant cells.

(A) Image of MyoB1-TM and VirE2. (B) Image of MyoB3-TM and VirE2.

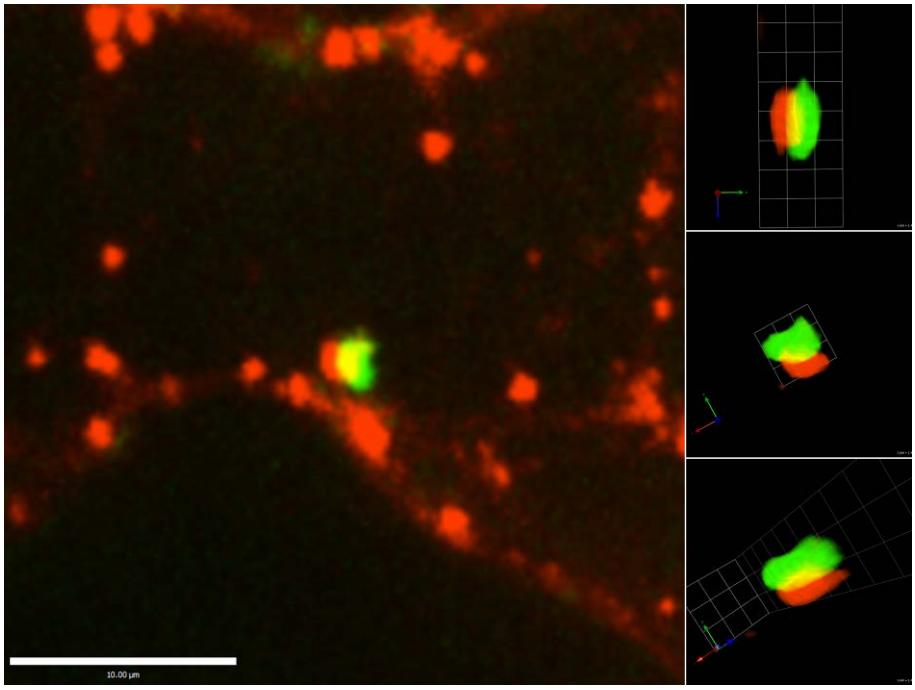

Figure 4- 8 3D reconstruction of co-expression of VirE2 and MyoB1-TM.

4.3.2 Effect of overexpressing DUF593 on VirE2 motility

Previous study (Peremyslov *et al.* 2013) identified the function of DUF593 domains, which exist in MyoB transmembrane proteins. MyoB proteins are able to interact with myosin XI via direct binding between DUF593 and the myosin GTD. Assuming that myosin XI are capable of transporting VirE2 along actin filament, the overexpression of DUF593 should efficiently stop the motion of VirE2 in plant cells.

To track DUF593 under confocal microscopy, coding sequence of DUF593 from MyoB1 and MyoB2 was fused with mCherry firstly. *Agrobacterium tumefaciens* bearing mCherry tagged DUF593 was infiltrated into *Nicotiana benthamiana* leaves.

Figure 4-9 showed the expression of DUF593-1 (Figure 4-9A) and DUF593-2 (Figure 4-9B). DUF593-1 seems clustered and aggregated near cell periphery, while DUF593-2 showed more diffusion pattern. Both constructs were expressed with high levels as examined in light of the fluorescence intensity.

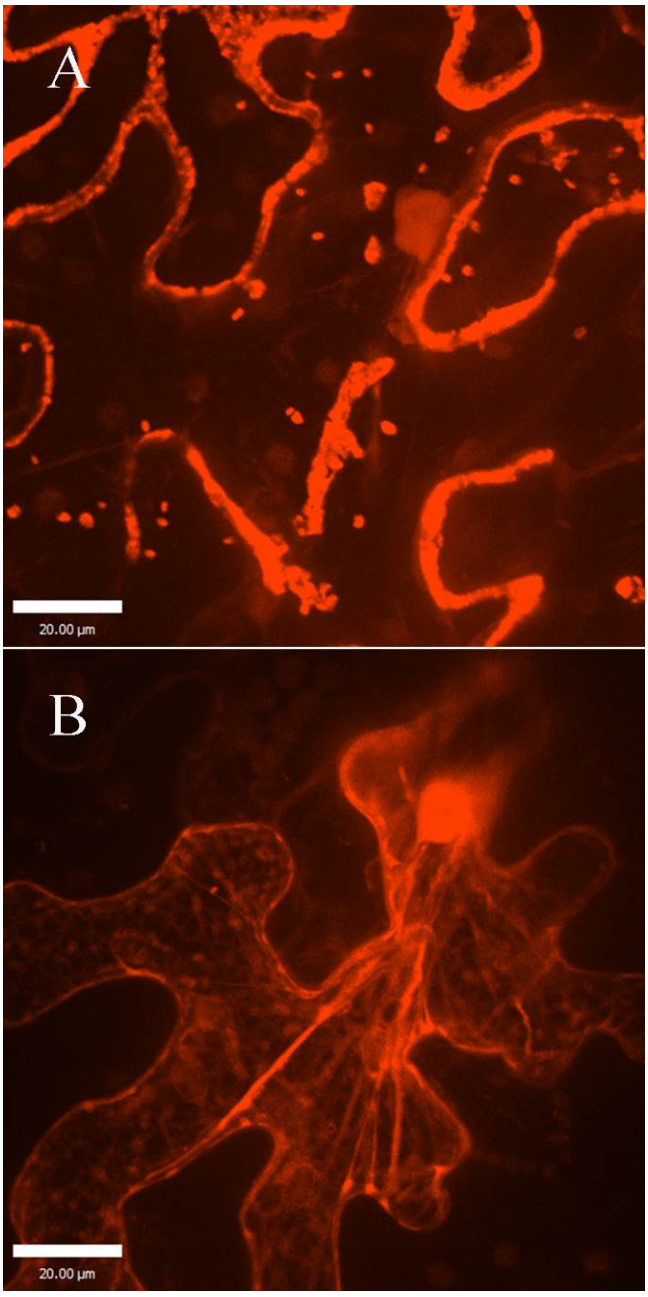

Figure 4- 9 Image of plant cells overexpressing DUF593 by confocal microscopy.

(A) Overexpression of DUF593-1. (B) Overexpression of DUF593-2.

To analyze whether the overexpression of DUF593 could stop or inhibit the motion of VirE2 in plant cells, *Agrobacterium tumefaciens*, bearing DUF593 on a binary vector and GFP tagged VirE2 on the Ti plasmid, was infiltrated into *Nicotiana benthamiana* leaves. Confocal microscopy was employed to visualize the fluorescence signals.

The left column of Figure 4-10 showed the image and trafficking pattern of VirE2 with overexpression of DUF593-1. GFP tagged VirE2 are successfully expressed as shown in Figure 4-10A. With the overexpression of DUF593-1, the feature of VirE2 has no change when compared with that without the overexpression of DUF593 (empty vector control, EV), the right column of Figure 4-10.

The trafficking patterns of VirE2 with overexpression of DUF593-1 were shown in the left column of Figure 4-10B. More than 20 VirE2 were tracked to investigate the trafficking patterns. However, an unexpected outcome that the motion of VirE2 showed no obvious reduction was recorded. This result indicated that DUF593-1 cannot affect the motion of VirE2. In other words, overexpression of DUF593-1 failed to delink VirE2 and Myosins. This result did not demonstrate the involvement of MyoB in VirE2's intracellular trafficking, possibly because DUF593 alone could not

fulfill its interaction activity with myosins. Interestingly, VirE2 with the overexpression of DUF593-1 in this study showed prominent directionality. This may be caused by the blocking of partial cytoskeleton with the overexpression of DUF593-1.

The middle column of Figure 4-10 showed the image and trafficking pattern of VirE2 with overexpression of DUF593-2. The motility feature of VirE2 has no change either, when compared with the EV control.

The trafficking patterns of VirE2 with overexpression of DUF593-2 were shown in the middle column of Figure 4-10B. More than 20 VirE2 were likewise tracked to investigate the trafficking patterns. As well as VirE2 with overexpression of DUF593-1, the motion of VirE2 showed no obvious reduction in this assay. DUF593-2 also showed no obvious effect on the motion of VirE2. Besides, compared with the control and DUF593-1, VirE2 with the overexpression of DUF-593-2 showed prominent directionality, indicating that the part of cytoskeleton was blocked by the overexpression of DUF593-2.

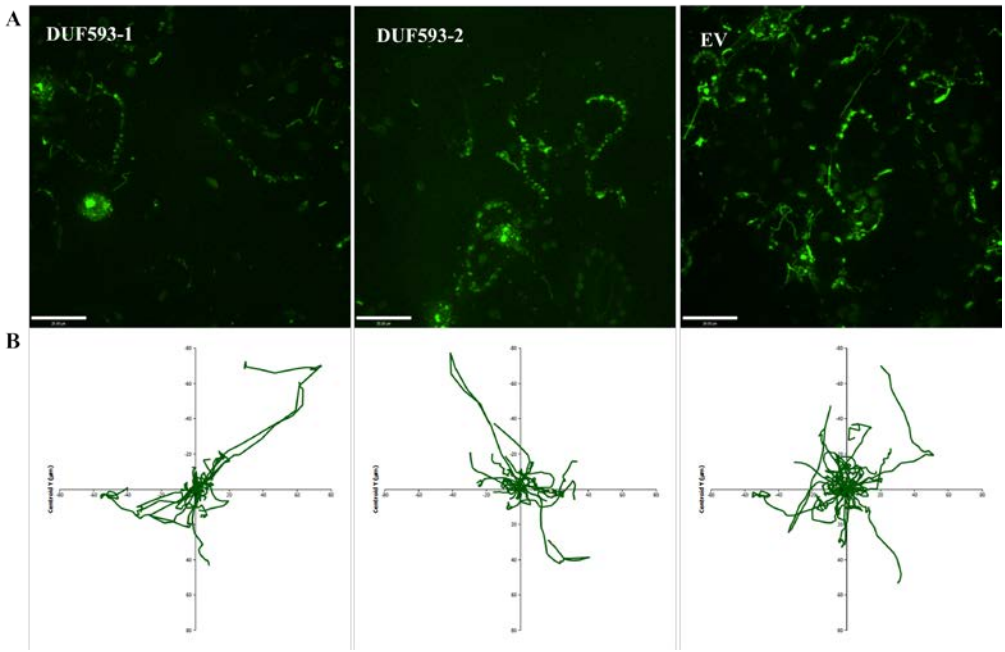

Figure 4- 10 Images and trafficking patterns of VirE2 with overexpression of DUF593 and empty vector control (EV).

(A) Image of VirE2 with overexpression of DUF593 and control by confocal microscopy. (B) Trafficking pattern of VirE2 with overexpression of DUF593 and control by Volocity software.

Figure 4-11 showed the mean velocities of VirE2 with different conditions. The mean velocity of VirE2 with no overexpression of DUF593, VirE2 with overexpression of DUF593-1 and VirE2 with overexpression of DUF593-2 is 0.433 μm/sec, 0.430 μm/sec and 0.417 μm/sec, respectively. Although compared with the EV control, the mean velocity of VirE2 with overexpression of DUF593 showed a little decrease, it is unreasonable to conclude that overexpression of DUF593 can interfere the motion of VirE2.

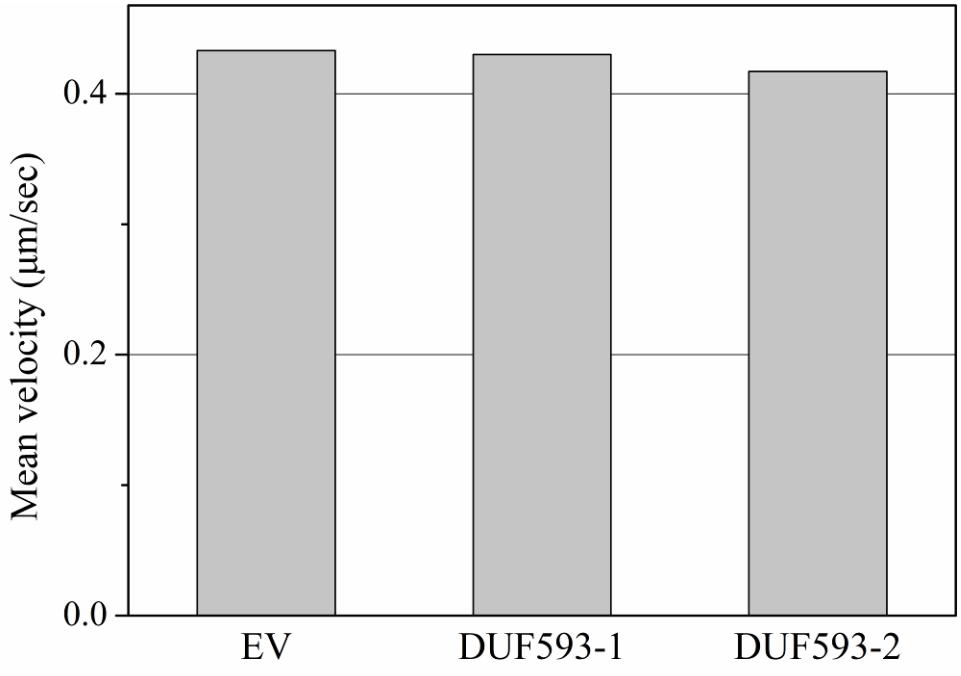

Figure 4- 11 Mean velocity of VirE2.

EV, empty vector control; DUF593-1, overexpressed DUF593-1; DUF593-2, overexpressed DUF593-2.

4.3.3 Mutation of MyoB2 in Arabidopsis abolished *Agrobacterium* - mediated transformation

To test the involvement of MyoB in *Agrobacterium*-mediated transformation, a strategy in genetic perspective was employed. Insertional mutants of Arabidopsis *myoB1* and *myoB2* were purchased from ABRC. Homozygous seeds were PCR-confirmed prior to germination. 10-day-old seedlings on MS agar plates were collected and their roots were cut into approximately 5 mm segments. These root segments were agroinfected with tumor inducing strain A348. Tumor formation after three weeks was shown in Figure 4-12A. As we can see, compared with wild type, *myoB2* showed a drastically effect in reduction of tumor numbers, while *myoB1* was not significant in such effect. The transformation efficiency as presented in the form of percentage is shown in Figure 4-12B. It shows that mutation in MyoB rendered Arabidopsis recalcitrant to *Agrobacterium*-mediated transformation. The efficiency of *myob2* was close to zero against around 60% of its wild type control. This result suggests that MyoB proteins, especially MyoB2, may play a critical role in *Agrobacterium*-mediated transformation.

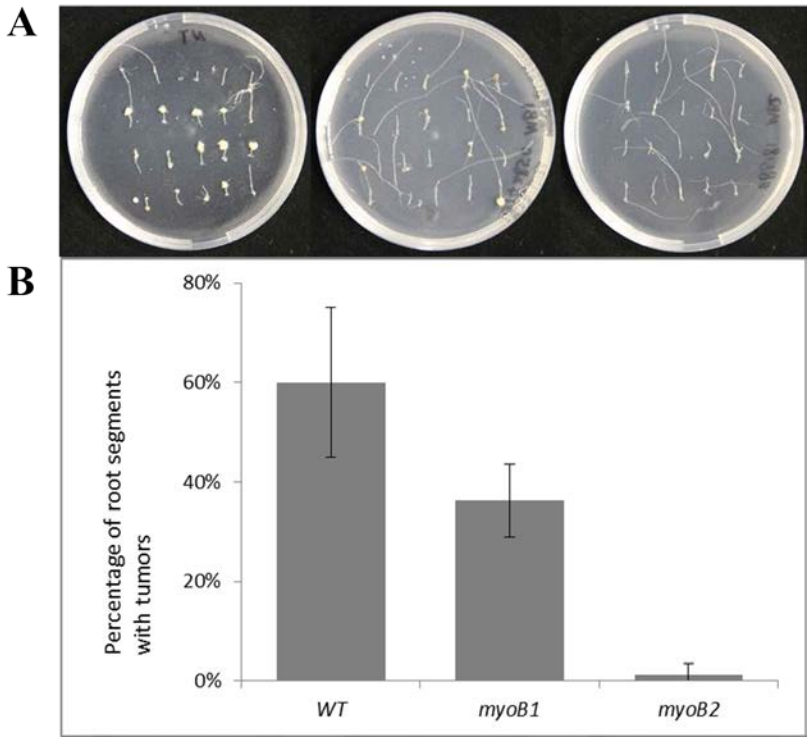

Figure 4- 12 Root tumorigenesis of MyoB mutants.

(A) left, WT, Col-0; middle, *myoB1*; right *myoB2* (B) Percentage of root segments with tumors.

5 DISCUSSION

5.1 VirE2 and organelle movements in plant cells

Most organelles in plant cells prefer to move through the cell rather than be anchored in place (Vick & A 2012). Cytoplasmic streaming is considered as the most famous form of organelle movement, the driving force of which is actomyosin system (Shimmen & Yokota 1994). Recently, in order to explain the mechanisms of cytoplasmic streaming, myosin proteins are getting more extensive attention of scientists. Among the myosin proteins, family of myosin XI is the most widely studied class (Tominaga *et al.* 2003; Vale 2003; Hammer & Sellers 2012; Buchnik *et al.* 2015). Moreover, fluorescent live-cell markers have made it possible to visualize the organelle movements. With this method, it is easy to reveal the characters of different organelles, and most studies have proved that organelles show saltatory motions (Collings *et al.* 2002; Jedd & Chua 2002).

In this report, we tried to analyze the relationship between VirE2 and plant cell organelles. Thus we used fluorescent markers (mCherry and GFP) to tag different organelles and VirE2. With the application of confocal microscopy and Volocity software, we successfully tracked the motions of VirE2 and four plant cell organelles (Golgi stacks, mitochondria,

peroxisomes and plastid), recorded their trafficking patterns, and calculated their velocities. Detailed analysis and comparison were conducted as well.

Among VirE2 and these four plant cell organelles, Golgi stacks reached the highest mean velocity, followed by VirE2. Peroxisomes showed moderated motility. The motilities of mitochondria and plastid were the weakest with almost no motion in this study. These different mean velocities among VirE2 and plant cell organelles may be determined by different functions of these constructs. Plant cells should be able to adjust the movement of various organelles by their own functions. However, organelle velocities can be easily affected by environment conditions, plant cell activity, species of plant, and so on. Thus the mean velocities in this study may be quite different with that in previous studies (Avisar *et al.* 2008; Peremyslov *et al.* 2008).

Besides the difference on mean velocity, the motions of Golgi stacks and peroxisomes showed obvious directional movement, vice versa VirE2. Considering that mitochondria and plastid showed no movement, we supposed that they localized in a specific site in plant cells. The directionality of organelle movement should be related to the growth phase of plant cells. Organelles such as Golgi stacks and peroxisomes should

participate in the metabolic process of plant cell. Moreover, plant cells with different growth phases have different requirements on organelles. Thus plant cell organelles showed directional movements. As for VirE2, it does not belong to the original system of plant cells. Therefore the plant cell could not adjust movement of VirE2. Thus VirE2 cannot show obvious directional movement.

5.2 Co-expression of MyoB-TM and VirE2

As mentioned above, myosin proteins are molecular motors in plant cells (Vale 2003). Among the superfamily of myosin, class of myosin XI is the largest. Myosin XI can bind actin microfilaments and hydrolyze ATP with its N-terminal head or motor domain (Vale 2003). Besides, the C-terminal of myosin XI possesses GTDs, which are utilized to bind various organelles as their cargoes (Reisen & Hanson 2007; Li & Nebenführ 2007).

The MyoB proteins have been proven to act as myosin XI receptors (Peremyslov *et al.* 2013). The DUF593 domain of MyoB can bind GTD of myosin XI. Thus MyoB and myosin XI together define a new class of transport vesicles. Considering that MyoB-TM displayed similar function as full length MyoB, we constructed MyoB-TM to investigate their

movements and functions. Occasionally, we found that the mean velocities of MyoB-TM were close to that of VirE2. Specifically, the mean velocity of VirE2 was between that of MyoB1-TM and that of MyoB3-TM. Thus we supposed that the movement of VirE2 could be affected by MyoB-TM and designed assays to test their co-expressions.

In this study, we concluded that most of the MyoB-TM could not co-localize VirE2. Compared with MyoB1-TM, MyoB3-TM seemed to be easier to co-localize VirE2. Reasons for this result could be in relation with their different movements. The trafficking patterns of MyoB1-TM were similar with that of plant cell organelles, all of which showed obvious directionalities. However, the trafficking patterns of MyoB3-TM were in line with that of VirE2, both of which showed random motions. The random distribution made it easier for MyoB3-TM to meet with VirE2 than MyoB1-TM. Therefore the co-localization between MyoB3-TM and VirE2 was easier to be visualized than that between MyoB1-TM and VirE2. It seemed that MyoB1-TM should prefer to co-localize plant cell organelles. Further study should be conducted to test this hypothesis.

5.3 Interfere VirE2 by overexpressing DUF593

DUF593 domain is a myosin binding domain in MyoB, which is responsible for binding the myosin XI-K GTD (Peremyslov *et al.* 2013). It is a coiled-coil domain highly conserved in plants (Holding *et al.* 2007). With this binding function of DUF593, MyoB proteins are successfully transformed to myosin XI acceptors. Specifically, according to the binding of DUF593 and GTD, MyoB proteins are connected to myosin XI proteins. Then the formed system acts as a class of efficient transport vesicles.

VirE2 is able to move along actin filament. Based on this factor, we supposed that myosin XI can act as the transport vesicles for VirE2. Then VirE2 should move along actin filament with the driving force of myosin XI. Therefore with the overexpression of DUF593, most of myosin XI should be occupied. Then sites for VirE2 binding should be reduced, and further the movement of VirE2 would dramatically decrease.

However, the results in this study seemed not to support this hypothesis. With overexpression of either DUF593-1 or DUF593-2, the motility of VirE2 showed no obvious change. Therefore, in this study, we concluded that overexpression of DUF593-1 failed to delink VirE2 and Myosins. This result did not demonstrate the involvement of MyoB in VirE2's intracellular

trafficking, possibly because DUF593 alone could not fulfill its interaction activity with myosins.

Despite that the overexpression of DUF593 could not interfere the movement of VirE2, it indeed interfered the distribution and directionality of VirE2 in plant cells. Without the overexpression of DUF593, the movement of VirE2 showed no dramatic directionality, and scattered all around the cell. When overexpressed DUF593, it seemed that VirE2 showed directionality to some extent, and the distribution of VirE2 seemed to be more concentrated. Reasons to cause this result should be complicated. However, the most prominent one should be that, with the overexpression of DUF593, part of cytoskeleton in plant cells would be blocked. Compared with VirE2 without competition from DUF593, the expressed VirE2 with competition from DUF593 in this study tended to be more concentrated and move in some smooth directions.

5.4 Tumorigenesis assay

To test the involvement of MyoB in *Agrobacterium*-mediated transformation, a strategy in genetic perspective was employed. The result showed that mutation in MyoB rendered Arabidopsis recalcitrant to

Agrobacterium-mediated transformation. Particularly, mutation in MyoB2 remarkably abolished *Agrobacterium*-mediated transformation of Arabidopsis. However, as illustrated above, with the overexpression of DUF593, the putative myosin-interacting domain of MyoB, the motility of VirE2 did not change much.

6 CONCLUSION

6.1 Different moving forms of VirE2 and organelles

VirE2 and plant cell organelles showed different moving velocities in this study. Their velocities were easily influenced by numerous factors including environment conditions, the type of plant and growth stage. For these reasons as well, the movement of same organelles in different plant would be quite different.

Except the organelles without movement, organelles moving with certain velocities exhibited apparent directionalities. However, VirE2 tended to scatter all around the cell. This is due to the fact that original organelles such as Golgi stacks and peroxisomes possess different functions. Thus they are assigned by plant cells to somewhere to play different roles. For example, Golgi stacks prefer to move around cell membrane while peroxisomes tend to assist the function of chloroplast. Then we visualized that they moved in certain directions in this study. Nevertheless, VirE2 are exogenous proteins for plant cells. Therefore their movements do not in line with plant cells. Thus VirE2 showed a scattered distribution in this study.

6.2 Inefficient co-localization of MyoB-TM and VirE2

Both MyoB1-TM and MyoB3-TM in this study localized in endoplasmic reticulum and exhibited same motion mode. They tended to move along endoplasmic reticulum.

Most of MyoB-TM did not co-localize with VirE2 in this study. Occasionally, some of MyoB-TM could co-localize with VirE2. And the co-localization could be confirmed by the 3D reconstruction, which indicated that MyoB-TM and VirE2 indeed co-localized together instead of an illusion of projection of different optical layers.

6.3 Inefficient interference to VirE2 with overexpression of DUF593

In this study, DUF593 preferred to accumulate and further aggregate in cytoskeleton in plant cells. However with the overexpression of DUF593, the motility of VirE2 did not change much. Thus the motility of VirE2 may not be related to that of myosin XI.

Compared with the motion of VirE2 without the overexpression of DUF593, that with the overexpression of DUF593 showed dramatic directionalities, indicating that the part of cytoskeleton might be blocked by the

overexpression of DUF593.

6.4 Abolished *Agrobacterium*-mediated transformation by mutation of MyoB2 in Arabidopsis

In this study, mutation in MyoB2 remarkably abolished *Agrobacterium* -mediated transformation of Arabidopsis, suggesting that MyoB2 may play a critical role in the transformation, presumably due to its impact on VirE2 trafficking.

However, as illustrated above, with the overexpression of DUF593, the putative myosin-interacting domain of MyoB, the motility of VirE2 did not change much. Thus the connection of MyoB with VirE2 remains to be further elucidated.

7 REFERENCES

Akiyoshi, D. E., Klee, H., Amasino, R. M., Nester, E. W., & Gordon, M. P. (1984). T-DNA of Agrobacterium tumefaciens encodes an enzyme of cytokinin biosynthesis. *Proceedings of the National Academy of Sciences, 81*, 5994-5998.

Avisar, D., Prokhnevsky, A. I., Makarova, K. S., Koonin, E. V., & Dolja, V. V. (2008). Myosin XI-K Is required for rapid trafficking of Golgi stacks, peroxisomes, and mitochondria in leaf cells of Nicotiana benthamiana. *Plant Physiology, 146*, 1098-1108.

Bertani, G. (1951). Studies on lysogenesis. I. The mode of phage liberation by lysogenic Escherichia coli. *Journal Of Bacteriology, 62*, 294-300.

Bohne, J., Yim, A., & Binns, A. N. (1998). The Ti plasmid increases the efficiency of Agrobacterium tumefaciens as a recipient in virB-mediated conjugal transfer of an IncQ plasmid. *Proceedings Of The National Academy Of Sciences Of The United States Of America, 95*, 7057-7062.

Buchnik, L., Abu-Abied, M., & Sadot, E. (2015). Role of plant myosins in motile organelles: Is a direct interaction required? *Journal of Integrative Plant Biology, 57*, 24-30.

Bundock, P., & Hooykaas, P. J. (1996). Integration of Agrobacterium tumefaciens T-DNA in the Saccharomyces cerevisiae genome by illegitimate recombination. *Proceedings of the National Academy of Sciences, 93*, 15273-15275.

Burns, D. L. (1999). Biochemistry Of Type Iv Secretion. *Current Opinion In Microbiology, 2*, 25-29.

Cangelosi, G. A. (1989). Role for corrected Agrobacterium tumefaciens ChvA protein in export of beta-1,3-glucan. *Journal Of Bacteriology, 171*, 1609-1615.

Cangelosi, G. A. (1990). Sugars Induce the Agrobacterium Virulence Genes

Through a Periplasmic Binding Protein and a Transmembrane Signal ProteinSugars Induce the Agrobacterium Virulence Genes Through a Periplasmic Binding Protein and a Transmembrane Signal Protein. *Proceedings of the National Academy of Sciences, 87*, 6708-6712.

Cangelosi, G. A., Best, E. A., Martinetti, G., & Nester, E. W. (1991). Genetic analysis of Agrobacterium. *Methods In Enzymology, 204*, 384.

Citovsky, V., Zupan, J., Warnick, D., & Zambryski, P. (1992). Nuclear localization of Agrobacterium VirE2 protein in plant cells. *Science, 256*, 1803-1805.

Collings, D. A., Jdi, H., Marc, J., Overall, R. L., & Mullen, R. T. (2002). Life In The Fast Lane: Actin-Based Motility Of Plant Peroxisomes. *Canadian Journal of Botany, 80*, 430-441.

Conti, E., Uy, M., Leighton, L., Blobel, G., & Kuriyan, J. (1998). Crystallographic Analysis of the Recognition of a Nuclear Localization Signal by the Nuclear Import Factor Karyopherin α. *Cell, 94*, 194-204.

Dutt, M., & Grosser, J. W. (2010). An embryogenic suspension cell culture system for Agrobacterium-mediated transformation of citrus. *Plant Cell Reports, 29*, 1251-1260.

Gardner, R. C., & Knauf, V. C. (1986). Transfer of Agrobacterium DNA to Plants Requires a T-DNA Border But Not the virE Locus. *Science, 231*, 725-727.

Gelvin, S. B. (1998). Agrobacterium VirE2 Proteins Can Form a Complex with T Strands in the Plant Cytoplasm. *Journal Of Bacteriology, 180*, 4300-4302.

Gelvin, S. B. (2003). Agrobacterium-mediated plant transformation: the biology behind the "gene-jockeying" tool. *Microbiology And Molecular Biology Reviews, 67*, 16-37.

Grange, W., Duckely, M., Husale, S., Jacob, S., Engel, A., & Hegner, M. (2008). VirE2: A Unique ssDNA-Compacting Molecular Machine. *Plos Biology, 96*, 36a.

Hammer, I. J. A., & Sellers, J. R. (2012). Walking to work: roles for class V myosins as cargo transporters. *NATURE REVIEWS MOLECULAR CELL BIOLOGY, 13*, 14-26.

Holding, D., Otegui, M., Li, B., Meeley, R., Dam, T. B., & Jung, R., *et al.*. (2007). The maize floury1 gene encodes a novel endoplasmic reticulum protein involved in zein protein body formation. *Plant Cell, 19*, 2569-2582.

Hooykaas, P. J., & Schilperoort, R. A. (1992). Agrobacterium and plant genetic engineering. *10 Years Plant Molecular Biology*. Springer Netherlands.

Hooykaas, P. J. J. (1989). Transformation of plant cells via Agrobacterium. *Plant Molecular Biology, 13*.

Howard, E. A., Zupan, J. R., Citovsky, V., & Zambryski, P. C. (1992). The VirD2 protein of A. tumefaciens contains a C-terminal bipartite nuclear localization signal: implications for nuclear uptake of DNA in plant cells. *Cell, 68*, 109-118.

Iannino, N. I. Ó. D. (1998). Molecular Cloning and Characterization of cgs, the Brucella abortus Cyclic β(1-2) Glucan Synthetase Gene: Genetic Complementation of Rhizobium meliloti ndvB and Agrobacterium tumefaciens chvB Mutants. *Journal Of Bacteriology, 180*, 4393-4400.

Jasper, F., & Steinbiss, H. H. (1994). Agrobacterium T-Strand Production in vitro: Sequence-Specific Cleavage and 5' Protection of Single-Stranded DNA Templates by Purified VirD2 Protein. *Proceedings of the National Academy of Sciences, 91*, 694-698.

Jedd, G., & Chua, N. H. (2002). Visualization of peroxisomes in living plant cells reveals acto-myosin-dependent cytoplasmic streaming and peroxisome budding. *Plant & Cell Physiology, 43*, 384-392.

Jeon, G. A., Eum, J., & Sim, W. S. (1998). The role of inverted repeat (IR) sequence of the virE gene expression in Agrobacterium tumefaciens pTiA6. *Molecules And Cells, 8*, 49-53.

Kessler, F., & Schnell, D. J. (2006). The function and diversity of plastid protein import pathways: a multilane GTPase highway into plastids. *Traffic, 7*, 248-257.

Komari, T., Hiei, Y., Ishida, Y., Kumashiro, T., & Kubo, T. (1998). Advances in cereal gene transfer. *Current Opinion In Plant Biology, 1*, 161-165.

Kuehnle, A. R., Sugii, N., Kuehnle, A. R., & Sugii, N. (1991). Induction of Tumors in Anthurium andraeanum by Agrobactemium tumefaciens. *Hortscience*, 1325-1328.

Li, J. F., & Nebenführ, A. (2007). Organelle targeting of myosin XI is mediated by two globular tail subdomains with separate cargo binding sites. *Journal Of Biological Chemistry, 282*, 20593-20602.

Li, X., Yang, Q., Tu, H., Lim, Z., & Pan, S. Q. (2013). Direct visualization of Agrobacterium-delivered VirE2 in recipient cells. *Plant Journal, 77*, 487-495.

Liu, L., Zhou, J., & Pesacreta, T. C. (2001). Maize myosins: Diversity, localization, and function. *Cell Motility & the Cytoskeleton, 48*, 130-148.

Mayerhofer, R., Koncz-Kalman, Z., Nawrath, C., Crameri, A., Angelis, K., & Hohn, B.. (1991). T-DNA integration: a mode of illegitimate recombination in plants. *Embo Journal, 10*, 697-704.

Millar, A. H. (2014). *Plant Mitochondria Biogenesis and Cellular Function.*, 1-15.

Mysore, K. S., Nam, J., & Gelvin, S. B. (2000). An Arabidopsis histone H2A mutant is deficient in Agrobacterium T-DNA integration. *Proceedings of the National Academy of Science, 97*, 948-953.

Peremyslov, V. V., Klocko, A. L., Fowler, J. E., & Dolja, V. V. (2012). Arabidopsis myosin XI-K localizes to the motile endomembrane vesicles associated with F-actin. *Front Plant Sci, 3*, 184.

Peremyslov, V. V., Morgun, E. A., Kurth, E. G., Makarova, K. S., Koonin, E. V., & Dolja, V. V. (2013). Identification of Myosin XI Receptors in

Arabidopsis Defines a Distinct Class of Transport Vesicles. *Plant Cell, 25*, 3023-3038.

Peremyslov, V. V., Prokhnevsky, A. I., Avisar, D., & Dolja, V. V. (2008). Two class XI myosins function in organelle trafficking and root hair development in Arabidopsis. *Plant Physiology, 146*, 1109-1116.

Pitzschke, A., & Hirt, H. (2010). New insights into an old story: Agrobacterium-induced tumour formation in plants by plant transformation. *Embo Journal, 29*, 1021-1032.

Ream, W. (1998). Import of Agrobacterium tumefaciens Virulence Proteins and Transferred DNA into Plant Cell Nuclei. *Sub-cellular biochemistry, 29*, 365-384.

Reisen, D., & Hanson, M. R. (2007). Association of six YFP-myosin XI-tail fusions with mobile plant cell organelles. *Bmc Plant Biology, 7*, 553-554.

Relic, B., Andjelkovic, M., Rossi, L., Nagamine, Y., & Hohn, B. (1998). Interaction of the DNA modifying proteins VirD1 and VirD2 of Agrobacterium tumefaciens: analysis by subcellular localization in mammalian cells. *Proceedings Of The National Academy Of Sciences Of The United States Of America, 95*, 9105-9110.

Sattarzadeh, A. (2013). Arabidopsis myosin XI sub-domains homologous to the yeast myo2p organelle inheritance sub-domain target subcellular structures in plant cells. *Plant Cell Biology, 4*, 407.

Sheng, J., & Citovsky, V. (1996). Agrobacterium-plant cell DNA transport: have virulence proteins, will travel. *The Plant Cell, 8*, 1699.

Shimmen, T., & Yokota, E. (1994). Physiological and Biochemical Aspects of Cytoplasmic Streaming. *International Review of Cytology*, 97-139.

Shimoda, N., Toyoda-Yamamoto, A., Aoki, S., & Machida, Y. (1993). Genetic evidence for an interaction between the VirA sensor protein and the ChvE sugar-binding protein of Agrobacterium. *Journal Of Biological Chemistry, 268*, 26553-26558.

Stahl, L. E., Jacobs, A., & Binns, A. N. (1998). The conjugal intermediate of plasmid RSF1010 inhibits Agrobacterium tumefaciens virulence and VirB-dependent export of VirE2. *Journal Of Bacteriology, 180*, 3934-3939.

Steck, T. R., Morel, P., & Kado, C. I. (1988). Vir box sequences in Agrobacterium tumefaciens pTiC58 and A6. *Nucleic Acids Research, 16*, 8736.

Sundberg, C. D., & Ream, W. (1999). The Agrobacterium tumefaciens Chaperone-Like Protein, VirE1, Interacts with VirE2 at Domains Required for Single-Stranded DNA Binding and Cooperative Interaction. *Journal Of Bacteriology, 181*, 6850-6855.

Tang, X. J., Hepler, P. K., & SP, S. (1989). Immunochemical and immunocytochemical identification of a myosin heavy chain polypeptide in Nicotiana pollen tubes. *Journal Of Cell Science, 92*, 569-574.

Thomashow, M. F. (1987). Identification of a new virulence locus in Agrobacterium tumefaciens that affects polysaccharide composition and plant cell attachment. *Journal Of Bacteriology, 169*, 3209-3216.

Tominaga, M., Kojima, H., Yokota, E., Orii, H., Nakamori, R., Katayama, E., Anson, M., Shimmen, T., & Oiwa, K. (2003). Higher plant myosin XI moves processively on actin with 35 nm steps at high velocity. *Embo Journal, 22*, 1264-1272.

Turkina, M. V., & Sokolov, O. I. (2001). Myosins Are Motor Proteins of the Actomyosin Motility System: Association with Membranes and with the Signal Pathways. *Russian Journal Of Plant Physiology, 48*, 681-692.

Vale, R. D. (2003). The molecular motor toolbox for intracellular transport. *CELL, 112*, 467-480.

Vick, J. K., & Nebenfuhr, A. (2012). Putting on the breaks: regulating organelle movements in plant cells(f). *Journal of Integrative Plant*

Biology, 54, 868-874.

Ward, D. V., & Zambryski, P. C. (2001). The six functions of Agrobacterium VirE2. *Proceedings of the National Academy of Sciences, 98*, 385-386.

Watson, B., Currier, T. C., Gordon, M. P., Chilton, M.D., & Nester, E. W. (1975). Plasmid required for virulence of Agrobacterium tumefaciens. *Journal Of Bacteriology, 123,* 255-264.

Winans, S. C. (1992.) Two-way chemical signaling in Agrobacterium-plant interactions. *Microbiological Reviews, 56*, 13-31.

Winans, S. C., Burns, D. L., & Christie, P. J. (1996). Adaptation of a conjugal transfer system for the export of pathogenic macromolecules. *Trends In Microbiology, 4*, 64-68.

Yokota, E., Ueda, S., Tamura, K., Orii, H., Uchi, S., Sonobe, S., Hara-Nishimura, I., & Shimmen, T. (2009). An isoform of myosin XI is responsible for the translocation of endoplasmic reticulum in tobacco cultured BY-2 cells. *Journal Of Experimental Botany, 60*, 197-212.

Zhang, X., & Hu, J. (2009). Two small protein families, DYNAMIN-RELATED PROTEIN3 and FISSION1, are required for peroxisome fission in Arabidopsis. *The Plant Journal, 57*, 146-159.

Zhu, M., Fang, T., Li, S., Meng, K., & Guo, D. (2015). Bipartite Nuclear Localization Signal Controls Nuclear Import and DNA-Binding Activity of IFN Regulatory Factor 3.. *Journal Of Immunology*.

Zupan, J. R., & Zambryski, P. (1995). Transfer of T-DNA from Agrobacterium to the plant cell. *Plant Physiology, 107*, 1041.